View Article Online / Journal Homepage / Table of Contents for this issue
Dynamic Article Links

Dalton Transactions

Cite this: *Dalton Trans.*, 2012, **41**, 14046

www.rsc.org/dalton

COMMUNICATION

# Structural and reactivity comparison of analogous organometallic Pd(III) and Pd(IV) complexes†

**Fengzhi Tang,[a] Fengrui Qu,[a] Julia R. Khusnutdinova,[a] Nigam P. Rath[b] and Liviu M. Mirica*[a]**

***Received 14th September 2012, Accepted 3rd October 2012***
**DOI: 10.1039/c2dt32127k**

Published on 04 October 2012. Downloaded by University of Waterloo on 21/10/2014 20:20:07.

**The tetradentate ligands $^{R}$N4 ($^{R}$N4 = *N,N′*-di-alkyl-2,11-diaza[3,3](2,6)pyridinophane, R = Me or iPr) were found to stabilize cationic ($^{R}$N4)PdMe$_2$ and ($^{R}$N4)PdMeCl complexes in both Pd$^{III}$ and Pd$^{IV}$ oxidation states. This allows for the first time a direct structural and reactivity comparison of the two Pd oxidation states in an identical ligand environment. The Pd$^{III}$ complexes exhibit a distorted octahedral geometry, as expected for a d$^7$ metal center, and display unselective C–C and C–Cl bond formation reactivity. By contrast, the Pd$^{IV}$ complexes have a pseudo-octahedral geometry and undergo selective non-radical C–C or C–Cl bond formation that is controlled by the ability of the complex to access a five-coordinate intermediate.**

## Introduction

The role of Pd$^0$/Pd$^{II}$ intermediates in palladium-catalyzed reactions has been studied extensively for the past four decades.[1] In addition, Pd$^{IV}$ and Pd$^{III}$ complexes have recently been proposed as catalytically active intermediates in various oxidative organic transformations that complement the conventional Pd$^{0/II}$ catalysis.[2] In this context, development of ligand systems that can stabilize both Pd$^{III}$ and Pd$^{IV}$ complexes in a similar coordination environment can provide key insight into the mechanism of these important catalytic transformations,[3] especially for systems in which either one or both oxidation states have been proposed to be responsible for the observed reactivity.[4]

We have recently reported the first mononuclear organometallic Pd$^{III}$ complexes – stabilized by a tetradentate ligand *N,N′*-di-*tert*-butyl-2,11-diaza[3,3](2,6)pyridinophane ($^{tBu}$N4), and studied their C–C bond formation reactivity.[5] We have also investigated the involvement of Pd$^{III}$ species in aerobically-induced C–C bond formation from Pd$^{II}$ precursors[6] and in Kharasch radical additions.[7] Continuing our study of high valent Pd chemistry, herein we report the use of *N*-methyl ($^{Me}$N4) and *N*-isopropyl ($^{iPr}$N4) pyridinophane ligand analogs that lead to the isolation and characterization of analogous mononuclear Pd$^{III}$ and Pd$^{IV}$ complexes. Isolation of these complexes enabled a direct structural and reactivity comparison of the two Pd oxidation states in an identical ligand environment.

## Results and discussion

### Synthesis and properties of Pd$^{III}$ and Pd$^{IV}$ complexes

The $^{Me}$N4 and $^{iPr}$N4 ligands were synthesized using reported and slightly modified synthetic procedures[8] and were used to prepare the Pd$^{II}$ precursors ($^{Me}$N4)Pd$^{II}$MeCl (**1**), ($^{iPr}$N4)Pd$^{II}$MeCl (**2**), ($^{Me}$N4)Pd$^{II}$Me$_2$ (**3**), and ($^{iPr}$N4)Pd$^{II}$Me$_2$ (**4**) (Scheme 1).[9] Cyclic voltammetry (CV) studies of complexes **1–4** in MeCN reveal two oxidation waves assigned to Pd$^{II}$/Pd$^{III}$ and Pd$^{III}$/Pd$^{IV}$ redox couples, respectively (Fig. 1 and Table 1).[5,9,10] Interestingly, these oxidation potentials increase with the increasing steric bulk of the ligand from $^{Me}$N4 to $^{iPr}$N4 to $^{tBu}$N4. For example, the

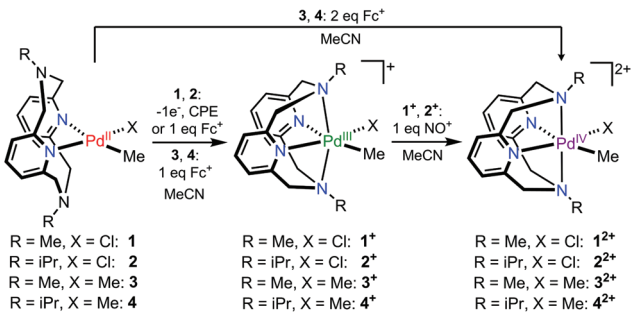


**Scheme 1** Synthesis of ($^{R}$N4)Pd$^{III}$ and ($^{R}$N4)Pd$^{IV}$ complexes.

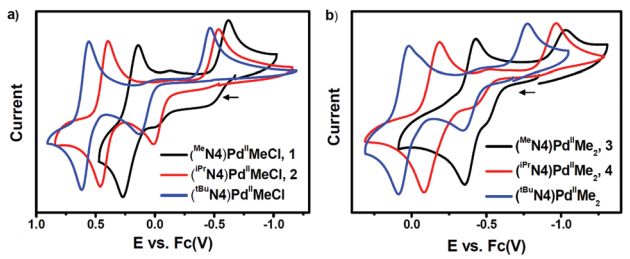


**Fig. 1** CVs of (a) $^{R}$N4Pd$^{II}$MeCl and (b) $^{R}$N4Pd$^{II}$Me$_2$ complexes. Conditions: 0.1 M Bu$_4$NClO$_4$–MeCN or CH$_2$Cl$_2$, 100 mV s$^{-1}$. The CV data for [($^{tBu}$N4)Pd$^{III}$MeCl]$^+$ were taken from ref. 5.

[a]*Department of Chemistry, Washington University, One Brookings Drive, St. Louis, Missouri 63130-489, USA. E-mail: mirica@wustl.edu*
[b]*Department of Chemistry and Biochemistry, University of Missouri-St. Louis, One University Boulevard, St. Louis, Missouri 63121-4400, USA*

† Electronic supplementary information (ESI) available. CCDC 884994. For ESI and crystallographic data in CIF or other electronic format see DOI: 10.1039/c2dt32127k


This journal is © The Royal Society of Chemistry 2012

View Article Online

Published on 04 October 2012. Downloaded by University of Waterloo on 21/10/2014 20:20:07.

**Table 1** Spectroscopic properties of $Pd^{III}$ complexes

| | $E_{pc}^{III/II}$, $E_{pa}^{II/III}$, $E_{1/2}^{III/IV}$ ($\Delta E_p$)[a] (mV) | UV-vis (MeCN), $\lambda$ (nm) ($\varepsilon$, $M^{-1}$ $cm^{-1}$) | EPR, $g_x$, $g_y$, $g_z$ ($A_N$, G)[b] |
|---|---|---|---|
| $\mathbf{1}^+$ | −620/−135, −480/−20,[c] +205 (130) | 606 (615), 475 (480), 316 (3550) | 2.212, 2.101, 2.014 (23.0) |
| $\mathbf{2}^+$ | −535, +10, +428 (65) | 658 (810), 517 (580), 312 (4020) | 2.228, 2.115, 2.011 (21.3) |
| $\mathbf{A}^{+d}$ | −464, +134, +587 (63) | 723 (1100), 545 (490), 368 (3300) | 2.239, 2.134, 2.005 (19.5) |
| $\mathbf{3}^+$ | −1030, −520, −395 (75) | 620 (405), 490 (430), 365 (1500) | 2.168 (16.0), 2.168 (16.0), 1.989 (22.5) |
| $\mathbf{4}^+$ | −965, −420, −135 (100) | 666 (623), 500 (500), 339 (4545) | 2.184 (15.0), 2.184 (15.0), 1.988 (20.4) |
| $\mathbf{B}^{+e}$ | −774, −341, +53 (67) | 741 (360), 560 (160), 350 (2300) | 2.222 (12.0), 2.191 (13.8), 1.986 (18.0) |

[a] Measured for $Pd^{II}$ precursors by CV *vs.* $Fc^+$/Fc in 0.1 M $Bu_4NClO_4$–MeCN or $CH_2Cl_2$, scan rate 100 mV $s^{-1}$; $\Delta E_p$ is the peak potential separation for the $Pd^{III/IV}$ couple. [b] In 3 : 1 PrCN : MeCN, 77 K; $A_N$'s are superhyperfine coupling constants to the axial N atoms. [c] The duplicate $E_{pa}^{II/III}$ and $E_{pc}^{II/III}$ values are likely due to two conformations present in solution (ref. 5). [d] CV and UV-vis data for $[(^{tBu}N4)Pd^{III}MeCl]^+$ ($\mathbf{A}^+$) are from ref. 5. [e] UV-vis and EPR data for $[(^{tBu}N4)Pd^{III}Me_2]^+$ ($\mathbf{B}^+$) are from refs. 5 and 6, respectively.

$E_{1/2}^{III/IV}$ values of $^{Me}N4$ complexes **1** and **3** are ~400 mV lower than those for the analogous $^{tBu}N4Pd^{II}$ complexes (Table 1).[5] The presence of such low $Pd^{III/IV}$ oxidation potentials and an appreciable separation between the $Pd^{II/III}$ and $Pd^{III/IV}$ potentials suggest that both $Pd^{III}$ and $Pd^{IV}$ species can be stabilized by $^{Me}N4$ and $^{iPr}N4$ (*vide infra*).

One-electron oxidation of $^{R}N4Pd^{II}MeCl$ complexes **1** and **2** by controlled potential electrolysis (CPE) in 0.1 M $Bu_4NClO_4$–MeCN or chemical oxidation with 1 equiv. ferrocenium hexafluorophosphate ($Fc^+PF_6^-$) generate the $Pd^{III}$ species $[(^{Me}N4)Pd^{III}MeCl]^+$ ($\mathbf{1}^+$) and $[(^{iPr}N4)Pd^{III}MeCl]^+$ ($\mathbf{2}^+$), while oxidation of **3** and **4** with 1 equiv. $Fc^+PF_6^-$ yields $[(^{Me}N4)Pd^{III}Me_2]^+$ ($\mathbf{3}^+$) and $[(^{iPr}N4)Pd^{III}Me_2]^+$ ($\mathbf{4}^+$), respectively (Scheme 1).[9] The X-ray structures of $[\mathbf{1}^+]ClO_4$, $[\mathbf{2}^+]ClO_4$, $[\mathbf{3}^+]ClO_4$, and $[\mathbf{4}^+]ClO_4$ all reveal the presence of the expected distorted octahedral geometry at the $d^7$ $Pd^{III}$ center (Fig. 2–4 and S33†).[10,11] Moreover, the Pd–$N_{axial}$ distances increase in ~0.05 Å steps when going from $^{Me}N4$ to $^{iPr}N4$ to $^{tBu}N4$ due to the increasing steric clash between the N-substituents and the equatorial ligands, as can be observed in the space filling models of the $Pd^{III}$ complexes (Fig. S33–S34). The presence of the less bulky N-substituent also leads to a more symmetric structure for the $Pd^{III}$ complexes. For example, while $\mathbf{3}^+$ exhibits a more symmetric $C_{2v}$ geometry, $\mathbf{4}^+$ has a $C_2$ symmetry due to the bulkier $^{iPr}N4$ ligand.[9]

The EPR spectra of complexes $\mathbf{1}^+$–$\mathbf{4}^+$ reveal anisotropic signals corresponding to $Pd^{III}$ centers with a $d_z^2$ ground state, as expected for a $d^7$ ion (Table 1, Fig. S28–S32†).[5,6,9,10] This is further supported by the presence of superhyperfine coupling to the two axial N atoms ($A_N$ = 12–23 G) that are observed in glassing solvent mixtures at 77 K.[9] Interestingly, the shorter Pd–$N_{axial}$ distances due to the size of the N-substituents are also responsible for the increasing trend in the $A_N$ superhyperfine coupling constants from $^{tBu}N4$ to $^{iPr}N4$ to $^{Me}N4$ (Table 1), suggesting that these EPR parameters can be used to approximate the strength of Pd–$N_{axial}$ interactions in $Pd^{III}$ complexes.[9] In addition, the same ligand steric effects likely lead to a red shift of the visible absorption bands with the increasing size of the N-substituent in $[(^{R}N4)Pd^{III}MeCl]^+$ and $[(^{R}N4)Pd^{III}Me_2]^+$ complexes (Table 1 and Fig. S23–S24†).[12]

Further chemical oxidation of $\mathbf{1}^+$ and $\mathbf{2}^+$ with 1 equiv. nitrosonium tetrafluoroborate ($NO^+BF_4^-$) in MeCN generates $[(^{Me}N4)Pd^{IV}MeCl]^{2+}$ ($\mathbf{1}^{2+}$) and $[(^{iPr}N4)Pd^{IV}MeCl]^{2+}$ ($\mathbf{2}^{2+}$), while treatment of **3** and **4** with 2 equiv. $Fc^+PF_6^-$ yields the $Pd^{IV}$ complexes $[(^{Me}N4)Pd^{IV}Me_2]^{2+}$ ($\mathbf{3}^{2+}$) and $[(^{iPr}N4)Pd^{IV}Me_2]^{2+}$ ($\mathbf{4}^{2+}$)

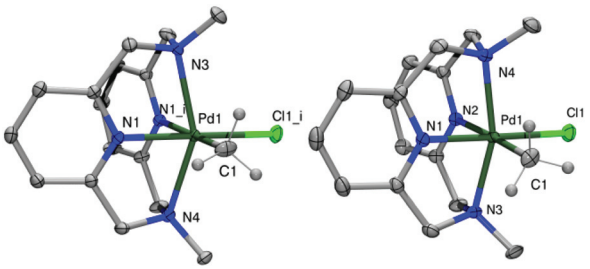


**Fig. 2** ORTEP representation (50% probability ellipsoids) of the cations of $[\mathbf{1}^+]ClO_4$ (left) and $[\mathbf{1}^{2+}](ClO_4)_2$ (right). Selected bond distances (Å) and angles (°): $[\mathbf{1}^+]ClO_4$, Pd1–C1 2.021(1), Pd1–Cl1i 2.344(3), Pd1–N1 2.085(2), Pd1–N1i 2.085(2), Pd1–N3 2.302(3), Pd1–N4 2.338(3), N3–Pd1–N4 149.12(1); $[\mathbf{1}^{2+}](ClO_4)_2$, Pd1–C1 2.072(2), Pd1–Cl1 2.2917(6), Pd1–N1 1.966(2), Pd1–N2 2.063(2), Pd1–N3 2.098(2), Pd1–N4 2.105(2), N3–Pd1–N4 158.94(7).

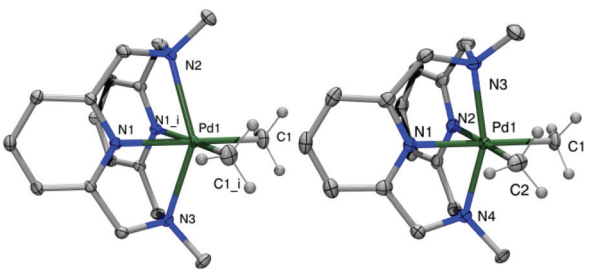


**Fig. 3** ORTEP representation (50% probability ellipsoids) of the cations of $[\mathbf{3}^+]ClO_4$ (left) and $[\mathbf{3}^{2+}](PF_6)_2$ (right). Selected bond distances (Å) and angles (°): $[\mathbf{3}^+]ClO_4$, Pd1–C1 2.0432(10), Pd1–C1i 2.0433(10), Pd1–N1 2.1393(7), Pd1–N1i 2.1393(7), Pd1–N2 2.4013 (11), Pd1–N3 2.3506(12), N2–Pd1–N3 145.37(4); $[\mathbf{3}^{2+}](PF_6)_2$, Pd1–C1 2.042(3), Pd1–C2 2.039(3), Pd1–N1 2.054(2), Pd1–N2 2.058(3), Pd1–N3 2.129(3), Pd1–N4 2.116(2), N3–Pd1–N4 156.70(10).

(Scheme 1).[9] The X-ray structures of $[\mathbf{1}^{2+}](ClO_4)_2$, $[\mathbf{3}^{2+}](PF_6)_2$, and $[\mathbf{4}^{2+}](PF_6)_2$ confirm the presence of $Pd^{IV}$ centers with a pseudo-octahedral geometry and reveal Pd–$N_{axial}$ distances that are 0.24–0.27 Å shorter than those in the $Pd^{III}$ analogs $\mathbf{1}^+$, $\mathbf{3}^+$, and $\mathbf{4}^+$, respectively (Fig. 2–4), in line with the preferred octahedral geometry for a $d^6$ $Pd^{IV}$ center *vs.* the distorted geometry of a $d^7$ $Pd^{III}$ ion.[10,11] Moreover, the $^{Me}N4$ ligand can easily accommodate the shorter Pd–$N_{axial}$ distances and the more compact structure of the octahedral $Pd^{IV}$ centers, as seen in the

View Article Online

Published on 04 October 2012. Downloaded by University of Waterloo on 21/10/2014 20:20:07.

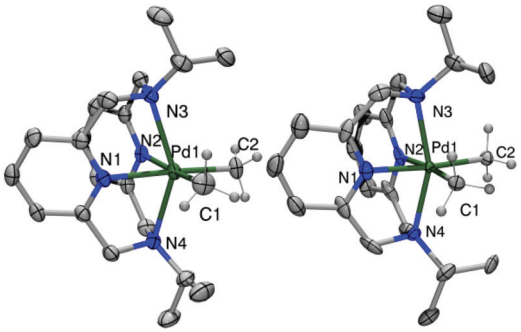


**Fig. 4** ORTEP representation (50% probability ellipsoids) of the cations of [**4**$^{+}$]$ClO_4$ (left) and [**4**$^{2+}$]$(PF_6)_2$ (right). Selected bond distances (Å) and angles (°): [**4**$^{+}$]$ClO_4$, Pd1–C1 2.033(4), Pd1–C2 2.042 (4), Pd1–N1 2.165(3), Pd1–N2 2.132(3), Pd1–N3 2.429(3), Pd1–N4 2.452(3), N3–Pd1–N4 145.61(11); [**4**$^{2+}$]$(PF_6)_2$, Pd1–C1 2.057(11), Pd1–C2 2.028(11), Pd1–N1 2.034(9), Pd1–N2 2.048(9), Pd1–N3 2.177(9), Pd1–N4 2.182(9), N3–Pd1–N4 155.5(3).

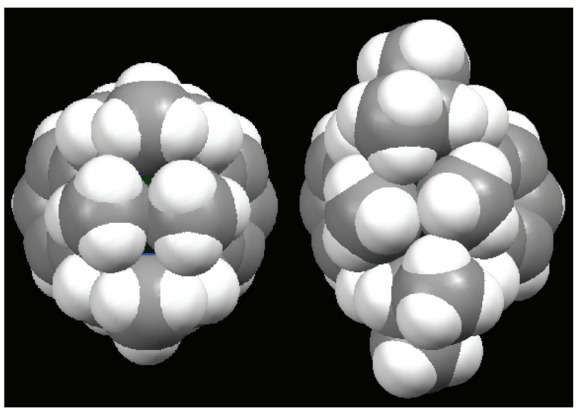

**Fig. 5** Space filling models of the cations of [**3**$^{2+}$]$(PF_6)_2$ and [**4**$^{2+}$]$(PF_6)_2$.

space filling models of **3**$^{2+}$ (Fig. 5). By contrast, the N-iPr groups of $^{iPr}$N4 in **4**$^{2+}$ cause a distortion of the macrocyclic ligand and push the Me ligands out of the equatorial plane to accommodate the shorter Pd–$N_{axial}$ distances of the $Pd^{IV}$ center (Fig. 5 and S36–S37†).[9] These structural properties also provide strong support for the observed trend of decreasing $Pd^{III/IV}$ oxidation potentials from $^{tBu}$N4 to $^{iPr}$N4 to $^{Me}$N4 (Fig. 1).[13] Interestingly, **1**$^{2+}$–**4**$^{2+}$ are uncommon dicationic organometallic complexes and are expected to exhibit increased electrophilic reactivity.[14,15]

### Reactivity comparison of $Pd^{III}$ and $Pd^{IV}$ complexes

The involvement of $Pd^{IV}$ and/or $Pd^{III}$ intermediates in various catalytic reactions has recently been demonstrated or proposed.[2] In this regard, our ability to isolate $Pd^{III}$ and $Pd^{IV}$ complexes in an identical ligand environment provides a unique opportunity to systematically probe their reactivity in organometallic reactions. The ($^{R}$N4)$Pd^{III}$MeCl complexes **1**$^{+}$ and **2**$^{+}$ are stable in the solid state or in solution in the dark, yet they undergo unselective and low-yielding C–C and C–Cl bond formation reactions in the

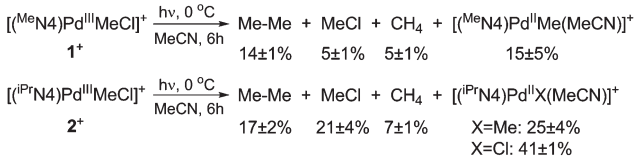


**Scheme 2** Reactivity of [($^{R}$N4)$Pd^{III}$MeCl]$^{+}$ complexes.[19]

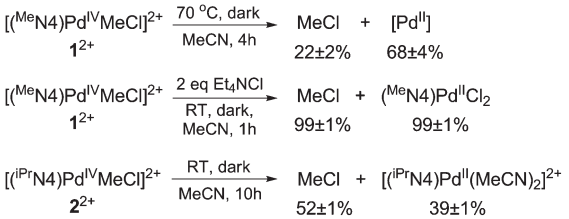


**Scheme 3** Reactivity of [($^{R}$N4)$Pd^{IV}$MeCl]$^{2+}$ complexes.[19]

presence of visible light to generate both ethane and methyl chloride in up to 17% and 21% yields, respectively (Scheme 2). Formation of the two products is suppressed completely in the presence of an effective alkyl radical trap, TEMPO,[9] suggesting a radical mechanism.[5] By contrast, the thermolysis of ($^{R}$N4)$Pd^{IV}$-MeCl complexes leads to selective formation of MeCl: **1**$^{2+}$ generates 22% MeCl in 4 h at 70 °C, while **2**$^{2+}$ undergoes reductive elimination even at RT to yield 52% MeCl (Scheme 3).[16] The observed reactivity is not affected by TEMPO, indicative of a non-radical mechanism. Moreover, addition of 2 equiv. $Cl^{-}$ to **1**$^{2+}$ leads to quantitative formation of MeCl and ($^{Me}$N4)$Pd^{II}Cl_2$ in 1 h at RT, suggesting an $S_N2$ reductive elimination mechanism.[17] The observed higher yield of MeCl for **2**$^{2+}$ *vs.* **1**$^{2+}$ is likely due to the greater steric bulk of the N-iPr *vs.* N-Me groups that facilitates formation of a five-coordinate intermediate *via* either chloride or axial amine dissociation.[18] Overall, these reactivity studies suggest that preferential formation of $Pd^{IV}$ *vs.* $Pd^{III}$ species during oxidatively-induced reactions leads to a selective C–Cl bond formation, likely due to the increased electrophilicity of $Pd^{IV}$ *vs.* $Pd^{III}$ centers in $S_N2$ reductive elimination.

Similar comparative reactivity studies were performed for the [($^{R}$N4)$Pd^{III}Me_2$]$^{+}$ and [($^{R}$N4)$Pd^{IV}Me_2$]$^{2+}$ species. Photolysis of the $Pd^{III}$ complexes **3**$^{+}$ and **4**$^{+}$ produces ethane in ~30% yield (Scheme 4).[16] Interestingly, the formation of ethane is only partially suppressed in the presence of TEMPO, suggesting the potential involvement of both radical and non-radical mechanisms (*vide infra*). By comparison, while almost no ethane is formed upon thermolysis of **3**$^{2+}$ at 70 °C, **4**$^{2+}$ generates up to 54% ethane *via* a non-radical mechanism (Scheme 5).[9] This dramatic reactivity difference may be due to the symmetric geometry of **3**$^{2+}$ that does not favor formation of a 5-coordinate intermediate, whereas the bulkier N-iPr groups lead to a geometric distortion in **4**$^{2+}$ that promotes the formation of a 5-coordinate intermediate necessary for ethane elimination.[18,20] In addition, photolysis of both **3**$^{2+}$ and **4**$^{2+}$ generates ethane in ~50% yield, both in the absence and presence of TEMPO, suggesting a non-radical mechanism of ethane formation. Therefore, we propose that a photo-induced dissociation of an axial N donor generates a 5-coordinate intermediate [($\kappa^{3\text{-}R}$N4)

 This journal is © The Royal Society of Chemistry 2012

View Article Online

Published on 04 October 2012. Downloaded by University of Waterloo on 21/10/2014 20:20:07.

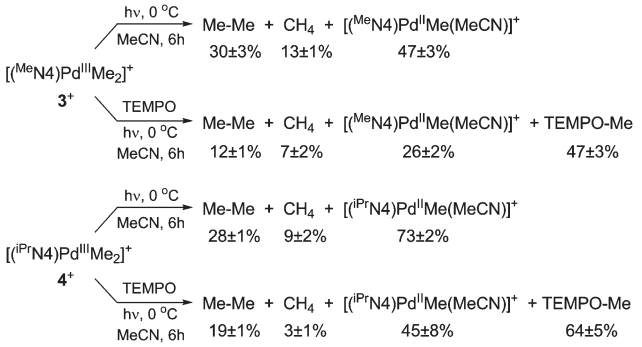


**Scheme 4** Reactivity of $[(^{R}N4)Pd^{III}Me_2]^+$ complexes.[19]

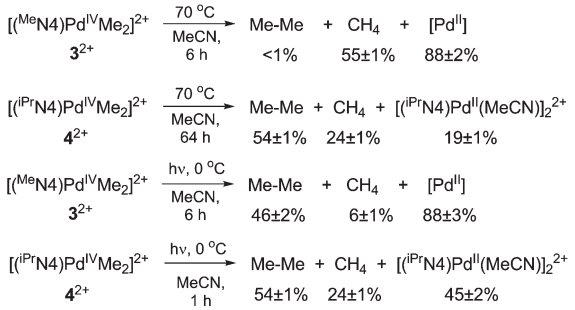


**Scheme 5** Reactivity of $[(^{R}N4)Pd^{IV}Me_2]^{2+}$ complexes.[19]

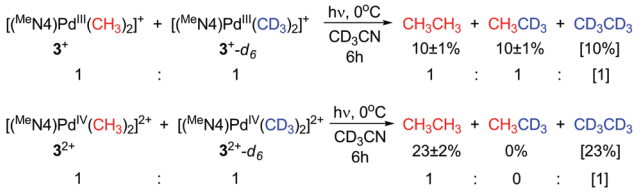


**Scheme 6** Crossover experiments for the photolysis of $\mathbf{3}^+$ and $\mathbf{3}^{2+}$.

$Pd^{IV}Me_2]^{2+}$, which is likely to undergo facile reductive elimination (*vide infra*).[18,20]

Crossover experiments were performed to gain insight into the possible mechanisms of ethane formation in the photolysis of $[(^{R}N4)Pd^{III}(Me)_2]^+$ and $[(^{R}N4)Pd^{IV}(Me)_2]^{2+}$ complexes. Photolysis of a 1 : 1 mixture of $[(^{Me}N4)Pd^{III}(CH_3)_2]ClO_4$, $[\mathbf{3}^+]ClO_4$, and $[(^{Me}N4)Pd^{III}(CD_3)_2]^+$, $[\mathbf{3}^+\text{-}d_6]ClO_4$, leads to formation of both $CH_3CH_3$ and $CH_3CD_3$ in 10% yield. Given the typical yield of ~30% ethane upon photolysis of $[\mathbf{3}^+]ClO_4$ under the same conditions, the result suggests a $CH_3CH_3 : CH_3CD_3 : CD_3CD_3$ ratio of 1 : 1 : 1 (Scheme 6). The observed ratio of ethane isotopologs is consistent with the formation of a $[(\kappa^{3\text{-}Me}N4)Pd^{IV}Me_3]^+$ intermediate ($\mathbf{5}^+$) that undergoes a fast rearrangement of the Me groups and thus can reductively eliminate any two of three Me groups.[6] In addition, the 1 : 1 : 1 ratio does not support a radical mechanism involving the coupling of two Me radicals or an $S_H2$-like mechanism involving a Me radical attacking the Me group of another $Pd^{III}$–Me molecule, as these mechanisms would lead to a 1 : 2 : 1 statistical ratio of ethane isotopologs.[21] The proposed intermediate $\mathbf{5}^+$ can be generated through a radical

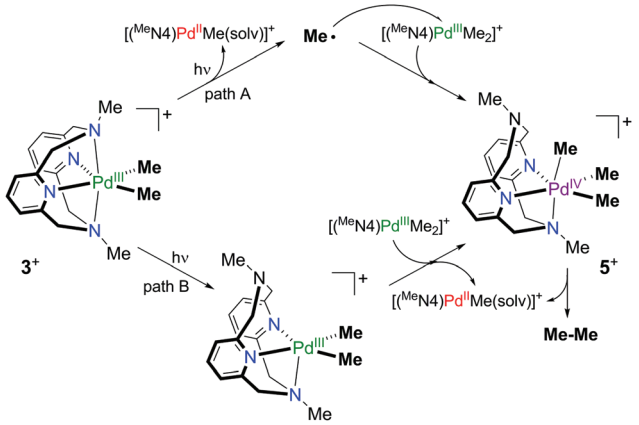


**Scheme 7** Proposed mechanisms for the photo-induced ethane elimination from $\mathbf{3}^+$ (and $\mathbf{4}^+$).

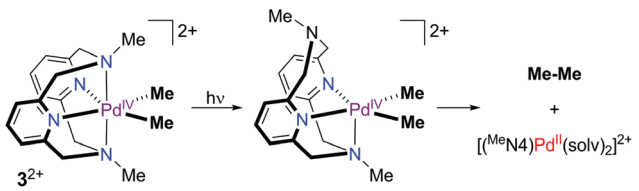


**Scheme 8** Proposed mechanism for the photo-induced ethane elimination from $\mathbf{3}^{2+}$ (and $\mathbf{4}^{2+}$).

mechanism involving a homolytic cleavage of a $Pd^{III}$–Me bond to form a Me radical that can subsequently bind to the $Pd^{III}$ center of another molecule of $\mathbf{3}^+$ (Scheme 7, path A).[5] Alternatively, a non-radical dissociation of an axial $Pd^{III}$–$N_{axial}$ bond upon irradiation can form a transient intermediate $[(\kappa^{3\text{-}Me}N4)Pd^{III}Me_2]^+$, which can undergo Me group transfer *via* disproportionation with another molecule of $\mathbf{3}^+$ to yield $\mathbf{5}^+$ (Scheme 7, path B).[6,22] The partial suppression of ethane formation by TEMPO suggests that both mechanisms may be operative during photolysis and can generate species $\mathbf{5}^+$, which is responsible for ethane formation.[22]

Interestingly, crossover studies for the $Pd^{IV}$ complexes yield different results. Photolysis of a 1 : 1 mixture of $[(^{Me}N4)Pd^{IV}(CH_3)_2](PF_6)_2$, $[\mathbf{3}^{2+}](PF_6)_2$, and $[(^{Me}N4)Pd^{IV}(CD_3)_2](PF_6)_2$, $[\mathbf{3}^{2+}\text{-}d_6](PF_6)_2$, yields 23% of $CH_3CH_3$, and no crossover product $CH_3CD_3$ is formed (Scheme 6).[9] Since the typical yield of ethane upon photolysis of $\mathbf{3}^{2+}$ is ~46%, the result suggests a 1 : 0 : 1 ratio of $CH_3CH_3$, $CH_3CD_3$, and $CD_3CD_3$. The observed ratio is consistent with a non-radical mechanism involving a photo-induced dissociation of an axial N donor to give the 5-coordinate intermediate, followed by rapid concerted reductive elimination of ethane (Scheme 8).[18,20] Overall, these reactivity studies suggest that, by contrast to $Pd^{III}$ analogs, the $Pd^{IV}$ complexes undergo selective C–C and C–heteroatom bond formation that most likely involve non-radical mechanisms.

## Conclusion

In summary, we have successfully isolated and characterized analogous organometallic $Pd^{III}$ and $Pd^{IV}$ complexes stabilized by

View Article Online

Published on 04 October 2012. Downloaded by University of Waterloo on 21/10/2014 20:20:07.

the tetradentate ligands $^{Me}$N4 and $^{iPr}$N4. The unprecedented isolation of both $Pd^{III}$ and $Pd^{IV}$ complexes with an identical ligand environment allowed a direct structural and organometallic reactivity comparison. The $d^7$ $Pd^{III}$ centers prefer a distorted octahedral geometry, while the $d^6$ $Pd^{IV}$ centers adopt a more compact octahedral geometry. In addition, reactivity studies show that $Pd^{III}$ centers lead to photo-induced radical formation and unselective C–C and C–Cl bond formation, although transient $Pd^{IV}$ intermediates can also be involved. By comparison, $Pd^{IV}$ centers undergo selective C–C or C–Cl bond formation through non-radical reductive elimination mechanisms. Overall, these studies suggest that both $Pd^{III}$ and $Pd^{IV}$ species could act as intermediates in various oxidatively-induced C–C and C–heteroatom bond formation reactions, while $Pd^{IV}$ centers tend to exhibit a more selective and higher yielding reductive elimination reactivity. Our current research efforts aim to provide insight into the involvement of $Pd^{III}$ and/or $Pd^{IV}$ species in stoichiometric and catalytic organic transformations employing high-valent Pd intermediates.

## Notes and references


1 (*a*) E. Negishi, *Handbook of Organopalladium Chemistry for Organic Synthesis*, John Wiley & Sons, Hoboken, NJ, 2002; (*b*) P. W. N. M. van Leeuwen, *Homogeneous Catalysis: Understanding the Art*, Kluwer Academic Publishers, Dordrecht, 2004; (*c*) J. F. Hartwig, *Organotransition Metal Chemistry: From Bonding to Catalysis*, University Science Books, Sausalito, 2010.

2 (*a*) A. Canty, *Dalton Trans.*, 2009, 10409; (*b*) X. Chen, K. M. Engle, D.-H. Wang and J.-Q. Yu, *Angew. Chem., Int. Ed.*, 2009, **48**, 5094; (*c*) K. Muniz, *Angew. Chem., Int. Ed.*, 2009, **48**, 9412; (*d*) T. W. Lyons and M. S. Sanford, *Chem. Rev.*, 2010, **110**, 1147; (*e*) P. Sehnal, R. J. K. Taylor and I. J. S. Fairlamb, *Chem. Rev.*, 2010, **110**, 824; (*f*) L.-M. Xu, B.-J. Li, Z. Yang and Z.-J. Shi, *Chem. Soc. Rev.*, 2010, **39**, 712; (*g*) D. C. Powers and T. Ritter, *Top. Organomet. Chem.*, 2011, **35**, 129.

3 D. C. Powers, E. Lee, A. Ariafard, M. S. Sanford, B. F. Yates, A. J. Canty and T. Ritter, *J. Am. Chem. Soc.*, 2012, **134**, 12002.

4 (*a*) W.-Y. Yu, W. N. Sit, K.-M. Lai, Z. Zhou and A. S. C. Chan, *J. Am. Chem. Soc.*, 2008, **130**, 3304; (*b*) T. S. Mei, X. S. Wang and J. Q. Yu, *J. Am. Chem. Soc.*, 2009, **131**, 10806; (*c*) K. M. Engle, T. S. Mei, X. S. Wang and J. Q. Yu, *Angew. Chem., Int. Ed.*, 2011, **50**, 1478.

5 J. R. Khusnutdinova, N. P. Rath and L. M. Mirica, *J. Am. Chem. Soc.*, 2010, **132**, 7303.

6 J. R. Khusnutdinova, N. P. Rath and L. M. Mirica, *J. Am. Chem. Soc.*, 2012, **134**, 2414.

7 J. R. Khusnutdinova, N. P. Rath and L. M. Mirica, *Angew. Chem., Int. Ed.*, 2011, **50**, 5532.

8 (*a*) F. Bottino, M. Di Grazia, P. Finocchiaro, F. R. Fronczek, A. Mamo and S. Pappalardo, *J. Org. Chem.*, 1988, **53**, 3521; (*b*) C. M. Che, Z. Y. Li, K. Y. Wong, C. K. Poon, T. C. W. Mak and S. M. Peng, *Polyhedron*, 1994, **13**, 771.

9 See ESI.†

10 L. M. Mirica and J. R. Khustnutdinova, *Coord. Chem. Rev.*, 2012, **256**, DOI: 10.1016/j.ccr.2012.04.030.

11 (*a*) A. J. Blake, A. J. Holder, T. I. Hyde and M. Schröder, *J. Chem. Soc., Chem. Commun.*, 1987, 987; (*b*) A. J. Blake, L. M. Gordon, A. J. Holder, T. I. Hyde, G. Reid and M. Schröder, *J. Chem. Soc., Chem. Commun.*, 1988, 1452; (*c*) A. R. Dick, J. W. Kampf and M. S. Sanford, *J. Am. Chem. Soc.*, 2005, **127**, 12790.

12 The detailed characterization of the observed spectroscopic trends for complexes $\mathbf{1}^+$–$\mathbf{4}^+$ is ongoing and will be reported elsewhere.

13 The $Pd^{IV}$ species $[(^{tBu}N4)Pd^{IV}MeCl]^{2+}$ can be generated electrochemically at low temperatures, yet it is unstable at RT (ref. 6).

14 Only one other dicationic organometallic complex has been reported to date: W. Oloo, P. Y. Zavalij, J. Zhang, E. Khaskin and A. N. Vedernikov, *J. Am. Chem. Soc.*, 2010, **132**, 14400.

15 While a few monoaryl $Pd^{IV}$ complexes have been isolated to date (T. Furuya and T. Ritter, *J. Am. Chem. Soc.*, 2008, **130**, 10060; N. D. Ball and M. S. Sanford, *J. Am. Chem. Soc.*, 2009, **131**, 3796; P. L. Arnold, M. S. Sanford and S. M. Pearson, *J. Am. Chem. Soc.*, 2009, **131**, 13912; Ref. 14), only one other monoalkyl $Pd^{IV}$ complex has been reported: D. Shabashov and O. Daugulis, *J. Am. Chem. Soc.*, 2010, **132**, 3965.

16 Thermolysis in the dark of $Pd^{III}$ complexes leads to unspecific decomposition and formation of methane. In addition, photolysis or thermolysis of $Pd^{II}$ precursors leads to formation of methane and Pd black, along with small amounts of ethane or MeCl.

17 (*a*) S. S. Stahl, J. A. Labinger and J. E. Bercaw, *Angew. Chem., Int. Ed.*, 1998, **37**, 2181; (*b*) B. S. Williams and K. I. Goldberg, *J. Am. Chem. Soc.*, 2001, **123**, 2576.

18 (*a*) J. M. Racowski, A. R. Dick and M. S. Sanford, *J. Am. Chem. Soc.*, 2009, **131**, 10974; (*b*) J. M. Racowski and M. S. Sanford, *Top. Organomet. Chem.*, 2011, **35**, 61.

19 During the reactivity studies for $^{R}N4Pd^{III}/Pd^{IV}$ complexes, the $^{R}N4Pd^{II}Me(solv)$ or $^{R}N4Pd^{II}(solv)_2$ products are unstable and lead to formation of methane and other $Pd^{II}$ products (see ESI†).

20 (*a*) J. Procelewska, A. Zahl, G. Liehr, R. van Eldik, N. A. Smythe, B. S. Williams and K. I. Goldberg, *Inorg. Chem.*, 2005, **44**, 7732; (*b*) D. M. Crumpton and K. I. Goldberg, *J. Am. Chem. Soc.*, 2000, **122**, 962.

21 M. P. Lanci, M. S. Remy, W. Kaminsky, J. M. Mayer and M. S. Sanford, *J. Am. Chem. Soc.*, 2009, **131**, 15618.

22 We have independently synthesized the $[(\kappa^{3\text{-}Me}N4)Pd^{IV}Me_3]^+$ species $\mathbf{5}^+$ and shown its involvement in aerobically-induced ethane elimination: F. Tang, Y. Zhang, N. P. Rath and L. M. Mirica, *Organometallics*, 2012, **31**, 6690–6696.


 This journal is © The Royal Society of Chemistry 2012